

Equalization Concepts for EDGE

Wolfgang H. Gerstacker, *Member, IEEE*, and Robert Schober, *Student Member, IEEE*

Abstract—In this paper, an equalization concept for the novel radio access scheme Enhanced Data rates for GSM Evolution (EDGE) is proposed by which high performance can be obtained at moderate computational complexity. Because high-level modulation is employed in EDGE, optimum equalization as usually performed in Global System for Mobile Communications (GSM) receivers is too complex and suboptimum schemes have to be considered. It is shown that delayed decision-feedback sequence estimation (DDFSE) and reduced-state sequence estimation (RSSE) are promising candidates. For various channel profiles, approximations for the bit error rate of these suboptimum equalization techniques are given and compared with simulation results for DDFSE. It turns out that a discrete-time prefilter creating a minimum-phase overall impulse response is indispensable for a favorable tradeoff between performance and complexity. Additionally, the influence of channel estimation and of the receiver input filter is investigated and the reasons for performance degradation compared to the additive white Gaussian noise channel are indicated. Finally, the overall system performance attainable with the proposed equalization concept is determined for transmission with channel coding.

Index Terms—EDGE, equalization, mobile communications, reduced-state trellis-based equalizers.

I. INTRODUCTION

CURRENTLY, third-generation (3G) mobile communication systems are in the phase of standardization. Two major approaches to 3G mobile communications have to be distinguished. The first one is the introduction of completely new radio access schemes, such as universal mobile telecommunications service (UMTS), which is based on wideband code-division multiple access (WCDMA). In addition, one is also interested in an evolution of the existing time-division multiple access (TDMA) standards Global System for Mobile Communications (GSM) and Industry Standard 136 toward significantly higher spectral efficiency. For this, a novel common physical layer, Enhanced Data rates for GSM Evolution (EDGE), will be introduced for both TDMA schemes. A detailed description of EDGE including features such as link adaptation, incremental redundancy protocol, etc., is given in [1] and [2]. EDGE improves spectral efficiency by applying the modulation format 8-ary phase-shift keying (8PSK) instead of binary Gaussian minimum-shift keying (GMSK), which is used in GSM. In order to enable a smooth transition from GSM to

EDGE, additional important system parameters such as symbol rate and burst duration remain unchanged.

This paper focuses on suitable equalization concepts for EDGE. For equalization, the modification of the modulation scheme is of high significance. Optimum equalization, i.e., maximum-likelihood (ML) sequence estimation (MLSE) based on the Viterbi algorithm (VA), which is used in GSM and IS-136, would require an excessive computational complexity and is not realizable with currently available digital signal processors (DSPs). Therefore, alternative equalization strategies have to be employed. In this paper, the applicability of reduced-state trellis-based equalizers to EDGE is investigated. Two algorithms belonging to this class of suboptimum equalizers are considered: delayed decision-feedback sequence estimation (DDFSE), introduced by Duel-Hallen and Heegard [3], [4], and reduced-state sequence estimation (RSSE), proposed by Qureshi and Eyuboğlu [5], [6] (see also [7]), which may be viewed as a generalization of DDFSE. Both schemes are well suited for implementation because of their high regularity in contrast to related reduced-state schemes like the M -algorithm [8] and similar schemes like that proposed by Foschini [9]. Also, in general, performance is significantly better than that of simpler schemes such as decision-feedback equalization (DFE) [10], [11] or linear equalization [12].

The performance of both schemes for the EDGE scenario is analyzed theoretically and by means of computer simulations. In order to enable a comparison with theoretical limits, also the performance of MLSE is determined. For this, the derived theoretical bit error rate (BER) expressions are essential because with currently available computer workstations, even a simulation of MLSE is impossible for EDGE.

In general, reduced-state equalization has only an advantageous tradeoff between performance and complexity, if the channel impulse response which has to be equalized has a minimum-phase characteristic [4] and [5]. Therefore, the influence of an additional discrete-time prefilter, which transforms the overall impulse response into its minimum-phase equivalent, on equalizer performance is analyzed. Also, the effects of different receiver input filters are considered.

This paper is organized as follows. In Section II, the discrete-time transmission model is introduced. DDFSE and RSSE are discussed in Section III. Here, also, strategies for prefilter calculation and approximations for the BERs of both schemes, which turn out to be quite accurate, are provided. In Section IV, detailed theoretical and simulation results are given for all relevant channel conditions for EDGE and the expected loss due to imperfect channel estimation is derived. Furthermore, the influence of the receiver input filter and the discrete-time prefilter, respectively, is analyzed. Also, statistics for the minimum Euclidean distance are presented by which some insight can be

Manuscript received December 6, 1999; revised June 10, 2000 and December 12, 2000; accepted May 20, 2001. The editor coordinating the review of this paper and approving it for publication is P. Driessen. This work was supported by Lucent Technologies Network Systems GmbH, Nürnberg, Germany.

W. H. Gerstacker is with Lehrstuhl für Nachrichtentechnik II, Universität Erlangen-Nürnberg, D-91058 Erlangen, Germany.

R. Schober is with the Department of Computer Engineering, University of Toronto, Toronto, ON M5S 3G4 Canada.

Publisher Item Identifier S 1536-1276(02)00191-5.

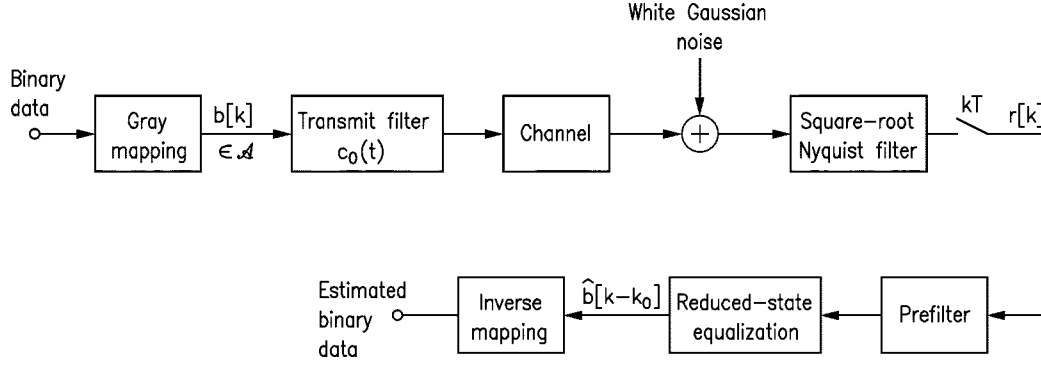


Fig. 1. Block diagram of the transmission model under consideration.

gained into the reasons for performance degradation compared to the additive white Gaussian noise (AWGN) channel. Finally, some simulation results for coded transmission with imperfect channel estimation are given.

II. TRANSMISSION MODEL

In the following, all signals are represented by their complex-valued baseband equivalents. Apart from Section IV-E, only uncoded transmission is considered. The block diagram of the system model is shown in Fig. 1. At the transmitter, in each time step, three bits of information are mapped onto 8PSK symbols $b[\cdot] \in \mathcal{A} = \{e^{j2\pi\nu/8} | \nu \in \{0, 1, \dots, 7\}\}$ using Gray encoding.¹ For transmit filtering, the linearized impulse $c_0(t)$ corresponding to GMSK with time-bandwidth product 0.3, which is the modulation format of GSM, is employed. Hence, the transmit filter impulse response is given by [13] and [14]

$$c_0(t) = \begin{cases} \prod_{i=0}^3 s(t + iT), & 0 \leq t \leq 5T \\ 0, & \text{else} \end{cases} \quad (1)$$

with

$$s(t) = \begin{cases} \sin\left(\pi \int_0^t g(\tau) d\tau\right), & 0 \leq t < 4T \\ \sin\left(\frac{\pi}{2} - \pi \int_0^{t-4T} g(\tau) d\tau\right), & 4T \leq t \leq 8T \\ 0, & \text{else} \end{cases} \quad (2)$$

where $T = 3.69 \mu\text{s}$ is the symbol duration. The Gaussian shaped frequency impulse $g(t)$ of duration $4T$ is given by

$$g(t) = \frac{1}{2T} \times \left(Q\left(2\pi \cdot 0.3 \frac{t - \frac{5T}{2}}{T\sqrt{\ln(2)}}\right) - Q\left(2\pi \cdot 0.3 \frac{t - \frac{3T}{2}}{T\sqrt{\ln(2)}}\right) \right) \quad \text{for } 0 \leq t \leq 4T \quad (3)$$

where $Q(\cdot)$ denotes the complementary Gaussian error integral

$$Q(t) = \frac{1}{\sqrt{2\pi}} \int_t^{+\infty} e^{-\tau^2/2} d\tau. \quad (4)$$

¹Actually, an additional rotation of the 8PSK symbols is performed in EDGE before transmit filtering [13]. However, the influence of this rotation on performance is negligible. Thus, for simplicity, it is not taken into account for the system model.

By this choice of the transmit filter, the transmit spectra of EDGE and GSM are approximately equal. Especially, the spectral masks of GSM are still fulfilled [15].

Because EDGE will use the same frequency bands as GSM, the same channel models can be used for system simulations and calculations. Thus, the channel profiles typical urban area (TU), rural area (RA), hilly terrain (HT), equalizer test (EQ), and static (ST) (no channel dispersion), which are specified in [16], are selected for numerical results. In order to facilitate calculations, it is assumed until Section IV-E that the channel is time-invariant during each burst,² which corresponds to low or moderate vehicle speeds, and the receiver has perfect knowledge of the channel impulse response.

For the receiver input filter, we assume a filter with square-root Nyquist frequency response. Two special cases meeting this condition are the whitened matched filter (WMF), which belongs to the class of optimum input filters [17], and the square-root raised cosine (SRC) filter [18]. Both will be considered for numerical results.

The (continuous-time) received signal is impaired by AWGN, which is characterized by the single-sided power spectral density N_0 . This corresponds to the test case of receiver sensitivity; the cases of cochannel and adjacent channel interference are not considered here.

The discrete-time received signal, sampled at times kT at the output of the receiver input filter, can be written as

$$r[k] = \sum_{\nu=0}^{L-1} d[\nu] b[k - \nu] + n[k]. \quad (5)$$

Here, $d[\nu]$, $0 \leq \nu \leq L - 1$ denote the coefficients of the combined discrete-time impulse response (CIR) of transmit filter, channel, and receiver input filter. L is the length of the CIR.³

The mean received energy per bit is given by

$$\bar{E}_b = \frac{\bar{E}_d}{\text{ld}(M)} \quad (6)$$

where $\text{ld}(\cdot)$ is the logarithm with base two, $M = 8$ is the alphabet size, and \bar{E}_d is defined as

$$\bar{E}_d = \mathbb{E} \left\{ \sum_{\nu=0}^{L-1} |d[\nu]|^2 \right\} \quad (7)$$

²In principle, it suffices to assume that the channel does not change within the path register length of the VA, if uncoded transmission is considered.

³In principle, the CIR is of infinite length. For definition of $d[\cdot]$, those L consecutive taps are selected, which exhibit maximum energy [19].

where $\mathbf{E}\{\cdot\}$ denotes expectation. Furthermore, a signal constellation with unit variance has been assumed for (6). The complex-valued zero-mean noise $n[\cdot]$ is Gaussian and white. This holds for the optimum WMF [17] and also for an SRC filter because the SRC filter autocorrelation function fulfills the first Nyquist criterion, i.e., it equals zero for $t = kT$, $k \in \mathbb{Z}$, $k \neq 0$ [18].

In front of reduced-state equalization, a prefilter is optionally inserted. The coefficients of the overall impulse response including the prefilter are denoted by $h[\nu]$, $0 \leq \nu \leq L-1$. It should be noted that ideal allpass prefiltering does neither change the channel length nor the channel energy, $\bar{E}_d = \bar{E}_h$. For convenience, the overall CIR is also represented by the vector

$$\mathbf{h} = [h[0] \ h[1] \ \dots \ h[L-1]]^T. \quad (8)$$

The estimated 8PSK symbols are denoted by $\hat{b}[k-k_0]$, where k_0 is the decision delay of the sequence estimator, which is given by the path register length of the VA. Finally, estimated bits are produced by an inverse mapping.

III. DDFSE AND RSSE

A. Characteristics of DDFSE and RSSE

EDGE receivers should be able to cope with the same channel conditions as GSM receivers. Thus, equalizers have to be tested for the GSM profiles mentioned in Section II. For the profiles HT and EQ, the discrete-time CIR has an effective length of $L = 7$, whereas for the remaining profiles, fewer taps are sufficient for an accurate characterization (e.g., $L = 4$ for TU). The length of the CIR together with the modulation format has a direct impact on the feasibility of equalization strategies.

In GSM, MLSE using the VA [17], which is the optimum equalizer in terms of sequence error probability, is widely employed [20], [21]. The computational complexity of MLSE is directly related to the number of states of the underlying trellis diagram, which is given by $Z = M^{L-1}$. Hence, MLSE has a maximum complexity of $Z = 2^6 = 64$ states for GSM. In contrast to that, complexity of MLSE is prohibitively high for EDGE. Even for TU, a full-state VA would require $Z = 512$ states, which is currently far too complex for a practical implementation. Thus, suboptimum equalizer concepts have to be considered for EDGE. In this paper, reduced-state trellis-based equalizers are discussed. Among the schemes in this class, DDFSE [3], [4] and RSSE [5]–[7] seem to be the most promising candidates because of their high regularity and good performance. Also, an extension of DDFSE and RSSE for generation of additional soft output is possible, which is highly desirable for subsequent channel decoding [20]–[22]. For this, the principles of reduced-state equalization and maximum-a-posteriori symbol-by-symbol estimation (MAPSSE) have to be combined, which is possible in a straightforward way [20], [21]. Two well-known MAPSSE schemes are the Bahl–Cocke–Jelinek–Raviv (BCJR) algorithm [23], performing a forward and a backward recursion (suited for block transmission), and the algorithm proposed by Lee [24], performing exclusively a forward recursion (suited for continuous transmission). Simulation results for channel decoding using

the reliability information provided by a soft-output RSSE are given in Section IV-E.

For DDFSE, only the first K , $1 \leq K \leq L$ taps of the CIR are used for definition of a trellis diagram with $Z = M^{K-1}$ states, whereas for the remaining taps per-survivor processing [25] is performed for metric calculations. For $K = 1$ and $K = L$, the limiting cases of DFE and MLSE, respectively, result.

With RSSE, an even finer tradeoff between performance and computational complexity is possible. For each tap delay i , $1 \leq i \leq L-1$, the signal constellation is partitioned into $N[i]$ subsets using Ungerboeck set partitioning and trellis states $S[k]$ are defined by the concatenation of the respective subset numbers $m[k-i]$, $1 \leq i \leq L-1$

$$S[k] \triangleq (m[k-1], m[k-2], \dots, m[k-L+1]). \quad (9)$$

In order to create a well-defined trellis, $N[1] \geq N[2] \geq \dots \geq N[L-1]$ has to be valid [5]. The number of states of the RSSE trellis is given by

$$Z = \prod_{i=1}^{L-1} N[i]. \quad (10)$$

For metric calculations, again per-survivor processing is applied. In the special case $N[1] = N[2] = \dots = N[K-1] = M$, $N[K] = N[K+1] = \dots = N[L-1] = 1$, DDFSE results. Here, for the first $K-1$ tap delays, each subset contains only one signal point, whereas for each of the last $L-K$ delays, only one subset exists, which is identical to the signal alphabet.

B. Prefiltering for DDFSE/RSSE

In order to obtain high performance, a minimum-phase CIR is essential for DDFSE and RSSE [4], [5]. Therefore, a discrete-time prefilter, which ideally has an allpass characteristic, should be introduced in front of equalization in order to transform the CIR into its minimum-phase equivalent. Whereas the optimum filter is recursive, for a practical implementation, a finite impulse response (FIR) approximation is of interest. For this, e.g., the minimum mean-squared error (MMSE) DFE feedforward filter is suited [26]–[28]. In the limit case of infinite filter order and infinite signal-to-noise ratio, the MMSE-DFE feedforward filter tends to the optimum prefilter. Hence, for filter orders that are not too small, a reasonable approximation can be expected. The MMSE-DFE filters can be calculated via the fast Cholesky factorization [27]–[29]. Recently, an even more efficient algorithm for FIR prefilter calculation based on a linear prediction (LP) approach has been proposed [30], [31]. Here, the FIR prefilter $F(z)$ of length L_f is realized as a cascade of two FIR filters

$$F(z) = A_1(z) \cdot A_2(z) \quad (11)$$

where $A_1(z)$ is a discrete-time matched filter, matched to the (estimated) channel impulse response, and $A_2(z)$ is a prediction-error filter of length L_2 designed for (approximately) whitening the output noise $n_1[\cdot]$ of $A_1(z)$. For calculation of $A_2(z)$, only the autocorrelation sequence of $n_1[\cdot]$ has to be known, which is proportional to the filter autocorrelation sequence of the discrete-time channel impulse response and

thus can be determined in a straightforward way. Then, the coefficients of $A_2(z)$ result from the Yule-Walker equations [31], which can be solved via the Levinson-Durbin algorithm [32]. It can be shown that the transfer function $F(z)$ tends to the transfer function of the ideal allpass filter for $L_f \rightarrow \infty$. For moderate finite filter orders, a reasonable approximation results [31].

The total number of required operations for this approach for prefilter computation is $(L_2 - 1)^2 + \mathcal{O}(L_2) + \mathcal{O}(L^2)$. It should be noted that the complexity of the MMSE-DFE approach is given by $c_1(L_f - 1)^2 + c_2(L_f - 1)(L - 1) + \dots$ and, thus, is also quadratic in the filter lengths, but the constants c_i are quite large [29]. This is in contrast to the LP approach, which seems to be preferable for a practical implementation. Using the LP approach, FIR prefilters with lengths up to $L_f \approx 25$ can be calculated in a practical receiver without violating the limitations imposed by a real-time environment.

C. Performance Analysis

For a fixed CIR \mathbf{h} , the BER of MLSE, DDFSE, and RSSE can be approximated by [4], [5], and [17]⁴

$$\text{BER} \approx C \cdot Q \left(\sqrt{\frac{d_{E,\min}^2(\mathbf{h})}{4\sigma_{n,I}^2}} \right). \quad (12)$$

Here, $Q(\cdot)$ is defined in (4) and $d_{E,\min}(\mathbf{h})$ is the minimum Euclidean distance being a function of the overall CIR (including prefilter, if applied), the modulation format, and the selected equalization algorithm. C is a constant factor, which is close to unity in most cases for the given channel profiles, modulation format, and mapping; therefore, C may be well approximated by one. $\sigma_{n,I}^2$ is the variance of inphase and quadrature component of $n[k]$

$$\sigma_{n,I}^2 = \frac{N_0}{2T}. \quad (13)$$

$d_{E,\min}(\mathbf{h})$ can be calculated using the Dijkstra algorithm [33]–[35], which performs a path search in the state transition diagram of the equalizer and is highly efficient for minimum-phase CIRs.⁵ It should be noted that the minimum phase property is no restriction in the case of MLSE because $d_{E,\min}(\mathbf{h})$ of MLSE does not depend on the channel phase, i.e., the CIR can be transformed into its minimum-phase equivalent before distance computation without loss of generality; in the case of DDFSE or RSSE, a minimum-phase CIR is required by any means for high performance (Section IV-A).

In our case of random, time-invariant channels, the BER expression of (12) has to be averaged

$$\text{BER} \approx \int \int \dots \int p(\mathbf{h}) Q \left(\sqrt{\frac{d_{E,\min}^2(\mathbf{h})}{4\sigma_{n,I}^2}} \right) d\mathbf{h}. \quad (14)$$

⁴In the cited references, an expression of the form of (12) is given only for the symbol error rate (SER). Nevertheless, it is straightforward to show that (12) is also valid for BER, with different constants C than for SER.

⁵An additional important attribute of the Dijkstra algorithm is that after convergence the exact minimum distance is available and not only an estimate, which is in contrast to some related schemes [36]–[38].

Here, $p(\mathbf{h})$ denotes the joint probability density function (pdf) of the coefficients of the overall CIR. In order to separate the influence of fading and intersymbol interference (ISI) on performance, the *normalized* minimum squared Euclidean distance $d_{\min}^2(\mathbf{h})$ [39], is introduced, with a normalization factor $2E_b/T$, where $E_b = E_h(\mathbf{h})/\text{ld}(M)$ is the mean received energy per bit for a given CIR \mathbf{h} with energy $E_h(\mathbf{h})$

$$d_{\min}^2(\mathbf{h}) = \frac{d_{E,\min}^2(\mathbf{h}) \cdot T}{\frac{2E_h(\mathbf{h})}{\text{ld}(M)}}. \quad (15)$$

With (6) ($\bar{E}_h = \bar{E}_d$ is valid), (13), and (15), we obtain for the quotient under the square root in (14)

$$\begin{aligned} \frac{d_{E,\min}^2(\mathbf{h})}{4\sigma_{n,I}^2} &= \frac{E_h(\mathbf{h})}{\bar{E}_h} d_{\min}^2(\mathbf{h}) \frac{\bar{E}_h}{\text{ld}(M)N_0} \\ &= \frac{E_h(\mathbf{h})}{\bar{E}_h} d_{\min}^2(\mathbf{h}) \frac{\bar{E}_b}{N_0}. \end{aligned} \quad (16)$$

Introducing (16) in (14) yields

$$\text{BER} \approx \int \int \dots \int p(\mathbf{h}) Q \left(\sqrt{\frac{E_h(\mathbf{h})}{\bar{E}_h} d_{\min}^2(\mathbf{h}) \frac{\bar{E}_b}{N_0}} \right) d\mathbf{h}. \quad (17)$$

In (17), for a given \mathbf{h} , the influence of ISI on BER is represented by the normalized squared Euclidean distance $d_{\min}^2(\mathbf{h})$ and that of fading by the energy ratio $E_h(\mathbf{h})/\bar{E}_h$. The pdf's of $d_{\min}^2(\mathbf{h})$ and $E_h(\mathbf{h})/\bar{E}_h$ for different channel profiles will be investigated in Section IV-D.

For the numerical results of Section IV, the multidimensional integral in (17) has been evaluated by Monte Carlo integration [40], i.e., $Q(\cdot)$ in (17) has been averaged over a sufficient number n of random channel realizations drawn from an ensemble with pdf $p(\mathbf{h})$,⁶ resulting in

$$\text{BER} \approx \frac{1}{n} \sum_{i=1}^n Q \left(\sqrt{\frac{E_h(\mathbf{h}_i)}{\bar{E}_h} d_{\min}^2(\mathbf{h}_i) \frac{\bar{E}_b}{N_0}} \right). \quad (18)$$

Here, $E_h(\mathbf{h}_i)$ and $d_{\min}^2(\mathbf{h}_i)$ denote the energy and the normalized minimum squared Euclidean distance of the overall CIR \mathbf{h}_i corresponding to the i th channel realization, respectively. It turned out that $n = 10000$ is sufficient for reliable results.

IV. NUMERICAL RESULTS

A. BER for Different Equalization Schemes and Channel Profiles

In Figs. 2–6, BERs are shown for all relevant channel profiles and equalization algorithms, assuming an SRC receiver input filter with rolloff factor $\alpha = 0.3$. The influence of different receiver input filters on performance will be examined later. We consider all possible DDFSE schemes including the special cases of DFE and MLSE, and three RSSE schemes, which are characterized by:

- 1) $N(1) = 2, N(2) = \dots = N(L - 1) = 1$, i.e., $Z = 2$ (denoted as RSSE2);

⁶Please note that here an explicit knowledge of the pdf is not required. Only the channel model has to be specified.

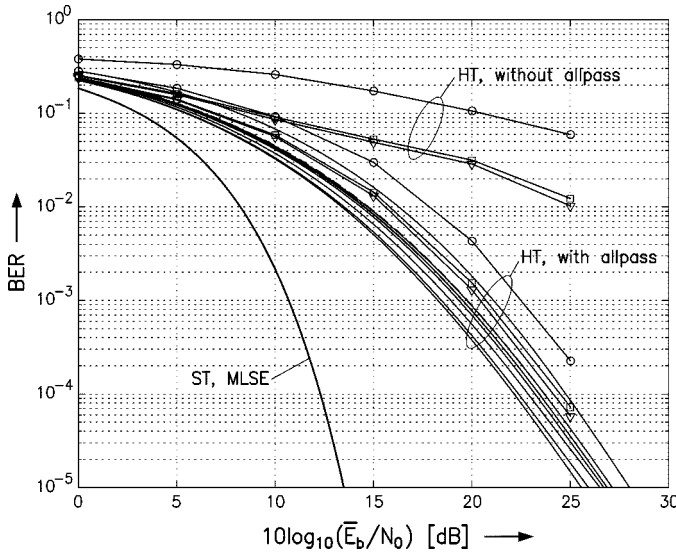


Fig. 2. BER versus $10 \log_{10}(\bar{E}_b/N_0)$ for different equalization schemes for HT profile (with and without allpass prefiltering). “—”: DDFSE (DFE-MLSE, BER improves as $K \in \{1, \dots, 7\}$ increases) (theory). “- -”: RSSE (RSSE2, RSSE4, RSSE2 \times 2) (theory). “o—o”: DDFSE ($K = 1$) (simulation). “□—□”: DDFSE ($K = 2$) (simulation). “∇—∇”: DDFSE ($K = 3$) (simulation).

- 2) $N(1) = 2, N(2) = 2, N(3) = \dots = N(L-1) = 1$, i.e., $Z = 4$ (denoted as RSSE2 \times 2);
- 3) $N(1) = 4, N(2) = \dots = N(L-1) = 1$, i.e., $Z = 4$ (denoted as RSSE4).

Mainly, calculated results are presented. For the DDFSE schemes ($K = 1, 2, 3$), a comparison to simulation results is made in order to verify our theoretical considerations.

The BERs for HT (Fig. 2) show that an allpass prefilter is mandatory for reduced-state schemes with moderate numbers of states. Without prefilter, a severe performance degradation occurs.⁷ Similar observations have also been made in [41] and [42], where it has been shown via analytically determined densities of zeros of the z transform of CIR $d[\cdot]$ that for the profiles HT, TU, and EQ, on average, a significant percentage of channel zeros lies outside the unit circle.

It should be noted that for the case of no prefiltering, only simulation results could be obtained because the Dijkstra algorithm did not converge for many channel realizations with non-minimum-phase CIR. With prefiltering, fast convergence could be observed for all considered channel profiles.

Because of the poor performance of reduced-state equalization without prefiltering, this case is not considered in the sequel. For each of the following results, ideal allpass filtering has been assumed. According to Fig. 2, with prefiltering, the loss of DDFSE ($K = 2$) compared to MLSE is limited to 1.6 dB for HT at $\text{BER} = 10^{-5}$; for $K = 3$ and $K = 4$, only slight improvements can be obtained compared to $K = 2$. Hence, $K = 2$ ($Z = 8$) seems to provide the best tradeoff between performance and complexity for DDFSE.

Obviously, calculated and simulated results for DDFSE in Fig. 2 are of the same order. The maximum difference is about 1.3 dB, mainly caused by error propagation, which plays a role

⁷This is also valid for TU and EQ, as has been proved by further simulations not shown in this paper.

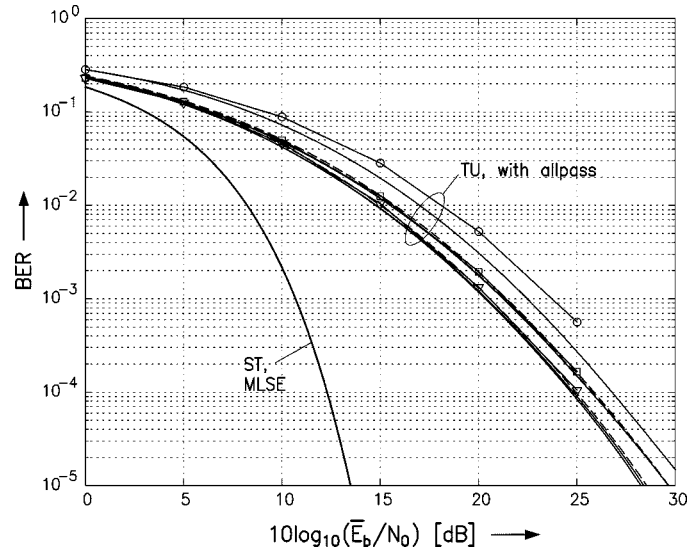


Fig. 3. BER versus $10 \log_{10}(\bar{E}_b/N_0)$ for different equalization schemes for TU profile (with allpass prefiltering). “—”: DDFSE (DFE-MLSE, BER improves as $K \in \{1, \dots, 7\}$ increases) (theory). “- -”: RSSE (RSSE2, RSSE4, RSSE2 \times 2) (theory). “o—o”: DDFSE ($K = 1$) (simulation). “□—□”: DDFSE ($K = 2$) (simulation). “∇—∇”: DDFSE ($K = 3$) (simulation).

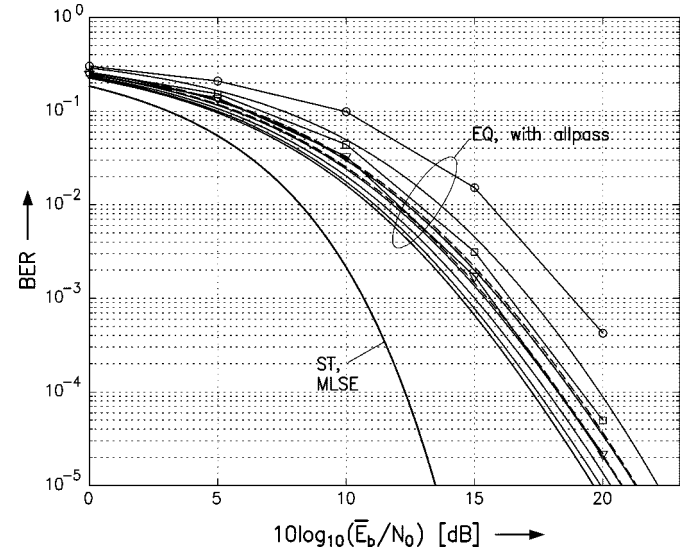


Fig. 4. BER versus $10 \log_{10}(\bar{E}_b/N_0)$ for different equalization schemes for EQ profile (with allpass prefiltering). “—”: DDFSE (DFE-MLSE, BER improves as $K \in \{1, \dots, 7\}$ increases) (theory). “- -”: RSSE (RSSE2, RSSE4, RSSE2 \times 2) (theory). “o—o”: DDFSE ($K = 1$) (simulation). “□—□”: DDFSE ($K = 2$) (simulation). “∇—∇”: DDFSE ($K = 3$) (simulation).

especially for small K and is not taken into account in the BER approximation of (17).

Among the considered RSSE schemes, RSSE2 \times 2 achieves the best performance for HT, which is essentially identical to that of DDFSE with $Z = 64$ ($K = 3$), whereas RSSE2 and RSSE4 perform as good as DDFSE with $Z = 8$ ($K = 2$). Thus, a further complexity reduction and performance improvement is possible by RSSE compared to DDFSE ($K = 2$). For comparison, the BER of the static (ST) channel equalized by MLSE is also included in Figs. 2–5.

Figs. 3 and 4 show BERs for the profiles TU and EQ, respectively. Simulated and calculated BERs agree even better than

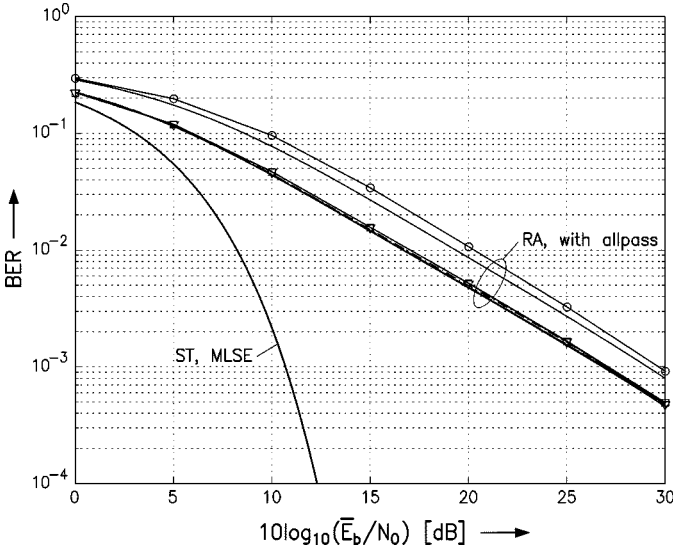


Fig. 5. BER versus $10 \log_{10}(\bar{E}_b/N_0)$ for different equalization schemes for RA profile (with allpass prefiltering). “—”: DDFSE (DFE-MLSE, BER improves as $K \in \{1, \dots, 7\}$ increases) (theory). “- -”: RSSE (RSSE2, RSSE4, RSSE2 \times 2) (theory). “o-o”: DDFSE ($K = 1$) (simulation). “□-□”: DDFSE ($K = 2$) (simulation). “▽-▽”: DDFSE ($K = 3$) (simulation).

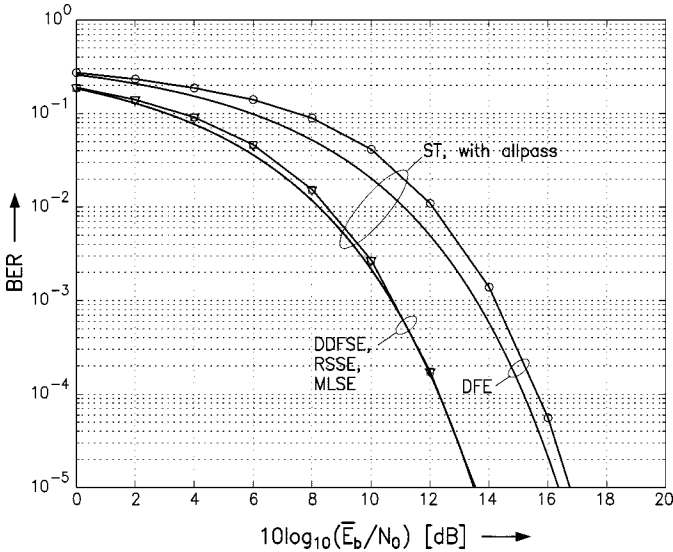


Fig. 6. BER versus $10 \log_{10}(\bar{E}_b/N_0)$ for different equalization schemes for ST profile (with allpass prefiltering). “—”: DDFSE (DFE-MLSE, BER improves as $K \in \{1, \dots, 7\}$ increases) (theory). “- -”: RSSE (RSSE2, RSSE4, RSSE2 \times 2) (theory). “o-o”: DDFSE ($K = 1$) (simulation). “□-□”: DDFSE ($K = 2$) (simulation). “▽-▽”: DDFSE ($K = 3$) (simulation).

for HT and DDFSE ($K = 2$) seems to be again the most favorable choice among the DDFSE schemes. As for HT, RSSE2 and RSSE4 perform as good as DDFSE ($K = 2$), while performance of DDFSE ($K = 3$) can be attained in principle by RSSE2 \times 2.

The BERs for RA (Fig. 5) show essentially a linear decrease over $10 \log_{10}(\bar{E}_b/N_0)$ because the RA profile resembles a flat Ricean fading channel with small Ricean factor. With all considered equalization schemes except for DFE, a performance similar to that of MLSE can be attained. This holds also for the ST channel Fig. 6. Furthermore, it is obvious from Fig. 6 that

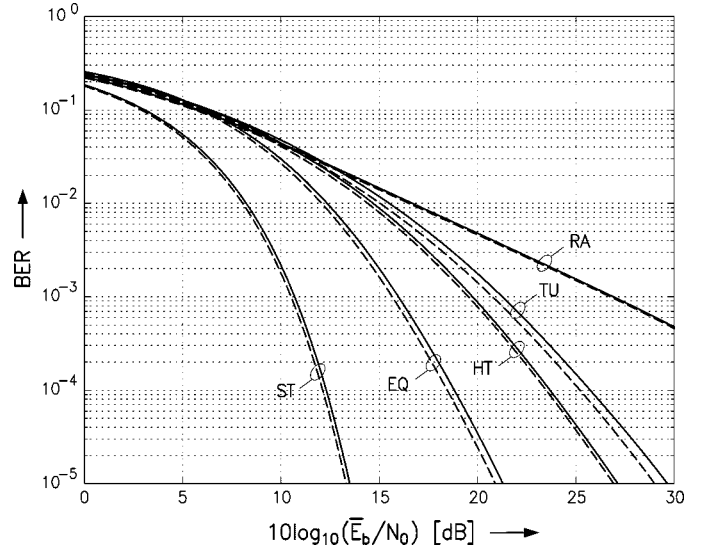


Fig. 7. BER versus $10 \log_{10}(\bar{E}_b/N_0)$ for DDFSE ($K = 2$) with additional allpass filtering for all profiles. “—”: SRC receiver input filter with $\alpha = 0.3$. “- -”: WMF.

the simulated BERs for DFE approach the theoretical curve for large \bar{E}_b/N_0 . This is due to the decreasing influence of error propagation.

For all profiles, a significant loss in performance compared to the ST channel can be observed. Because inherent path diversity is maximum for EQ and minimum for RA, these two profiles correspond to best (behind the reference case ST) and worst equalizer performance, respectively (Fig. 7).

B. Influence of Imperfect Channel Estimation

For the results of Section IV-A, the availability of error-free channel estimates at the receiver has been assumed. In a real system, DDFSE/RSSE has to rely on noisy channel estimates. For channel estimation, a standard ML approach is usually employed [43]–[45]. In GSM/EDGE, the specified training sequences guarantee an optimal noise suppression of ML channel estimation, if the length \hat{L} of the estimated CIR is limited to $\hat{L} \leq 6$ and $\hat{L} \geq L$ is valid. Then, the estimated channel coefficients are given by

$$\hat{h}[\kappa] = h[\kappa] + e[\kappa], \quad \kappa \in \{0, 1, \dots, \hat{L} - 1\} \quad (19)$$

where the estimation errors $e[\kappa]$ are Gaussian and mutually uncorrelated and have equal variances

$$\sigma_e^2 = \frac{\sigma_n^2}{N - \hat{L} + 1} \quad (20)$$

where N denotes the length of the training sequence, which is $N = 26$ for GSM/EDGE.

The influence of imperfect channel estimation on the quality of sequence estimation has been analyzed theoretically in [46]. An asymptotic upper bound on the BER of sequence estimation is presented in [46], according to which channel estimation errors are equivalent to losses in power efficiency of sequence estimation. If the sequence estimator requires $\bar{E}_b/N_0 = X$ for a given target BER in case of ideal channel knowledge, then

in case of ML channel estimation using optimum training sequences

$$\frac{\bar{E}_b}{N_0} = X \cdot \left(1 + \frac{\hat{L}}{N - \hat{L} + 1}\right) \quad (21)$$

is necessary for the target BER [46, eq. 10]. For $\hat{L} = 6$, $N = 26$

$$1 + \frac{\hat{L}}{N - \hat{L} + 1} = 1.29 \quad (22)$$

i.e., imperfect channel estimation results in an equivalent loss in power efficiency of ≈ 1.1 dB. For $\hat{L} > 6$, ML channel estimation results in correlated channel estimation errors. In this case, the performance loss due to channel estimation cannot be determined in a straightforward way.

After initial channel estimation, in general, channel tracking is necessary during sequence estimation in order to cope with the time variations of the CIR. Nevertheless, an additional performance loss due to the time variations of the CIR is inevitable and has to be determined via simulations Section IV-E. In general, an error floor occurs for nonideal channel tracking [47].

C. Influence of Receiver Input Filter

In the following, the influence of the receiver input filter on performance is examined. First, the performance of DDFSE ($K = 2$) with an SRC filter ($\alpha = 0.3$) and with a WMF, individually designed for each of the random channel realizations are compared. According to Fig. 7, differences are only small for each of the five profiles. For TU, a deviation of about 0.7 dB can be observed at $\text{BER} = 10^{-5}$ and for EQ, 0.4 dB at $\text{BER} = 10^{-5}$. For ST, RA, and HT, differences are even smaller. Further investigations showed that the gap between both cases is maximum (but still moderate) for DFE and decreases with increasing number of states of the trellis-based equalizer. This is because the WMF⁸ concentrates energy better in the first taps of the CIR than the combination of SRC and discrete-time allpass filter; concentration of energy is especially relevant for equalizers with few states.

Hence, a fixed SRC filter seems to be a near-optimum choice, while complexity is significantly lower than for the optimum WMF, which has to be continuously adapted. It should be noted that the frequency response of an optimum WMF often has a low-pass-like characteristic with a 3-dB cutoff frequency at $f \approx 1/(2T)$. This justifies the application of an SRC filter. Another frequently used suboptimum receiver input filter consists of the cascade of a matched filter, which is matched only to the transmit filter and a noise whitening filter. For the present application, we prefer the SRC filter because it is simpler to implement and offers a near-optimum performance.

Next, the influence of the rolloff factor α is analyzed. Fig. 8 shows BER curves for different rolloff factors α ; the results are valid for TU and DDFSE ($K = 2$). Obviously, BER decreases with decreasing α . The curves for $\alpha = 0.1$ and $\alpha = 0.3$ are almost identical.⁹ Similar results could also be obtained for the

⁸Here, the phase of the WMF is selected in that way that a minimum-phase overall CIR results.

⁹It should be mentioned that also for small rolloff factors such as $\alpha = 0.1$, $L = 7$ taps for the discrete-time CIR are sufficient in order to have only negligible taps for $k \geq L$ and $k < 0$, respectively.

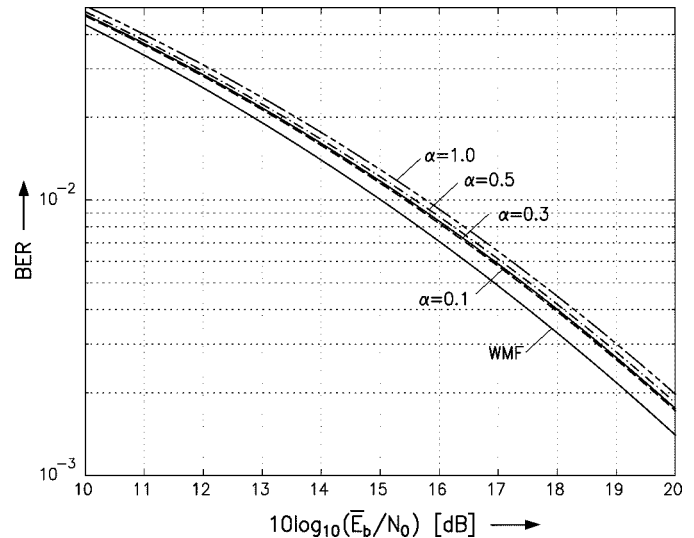


Fig. 8. BER versus $10\log_{10}(\bar{E}_b/N_0)$ for DDFSE ($K = 2$) with additional allpass filtering for TU profile and different receiver input filters (WMF and SRC with different α).

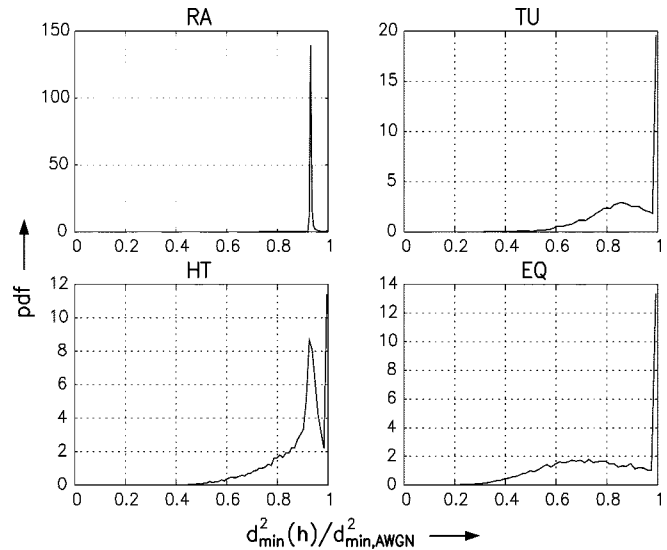


Fig. 9. Pdf's of $d_{\min}^2(\mathbf{h})/d_{\min, \text{AWGN}}^2$ for MLSE and different channel profiles.

remaining profiles and equalizers. Because a filter with $\alpha = 0.1$ is more difficult to implement in practice, $\alpha = 0.3$ is recommended.

D. Statistical Distribution of Minimum Euclidean Distance

Fig. 9 shows pdf's for the ratio $d_{\min}^2(\mathbf{h})/d_{\min, \text{AWGN}}^2$ for MLSE and the profiles RA, TU, HT, and EQ. For RA, the pdf reveals a sharp peak at 0.93. This can be verified, taking into account that RA in principle is identical to a flat fading scenario. Hence, $d_{\min, \text{RA}}^2(\mathbf{h})/d_{\min, \text{AWGN}}^2$ is essentially given by $d_{\min, \text{ST}}^2/d_{\min, \text{AWGN}}^2$. Via the Dijkstra algorithm, $d_{\min, \text{ST}}^2 = 0.8165$ could be obtained, whereas for the AWGN channel and 8PSK, $d_{\min, \text{AWGN}}^2 = 0.8787$ is valid [18]. This results in a ratio of approximately 0.93, i.e., an asymptotic loss of 0.32 dB.

For TU and EQ, the normalized Euclidean distance often is identical to that of the AWGN channel.¹⁰ In contrast, the pdf for HT has peaks at 1 and at 0.93. This can be explained as follows. For HT, paths with large delays have only small powers (in contrast to EQ), i.e., their amplitudes are often close to zero. For this case, CIRs similar to the RA case appear, causing the peak at 0.93. On the other hand, if these paths are not negligible, the CIR has a quite random shape, which implicates the peak at 1.0.

The pdf's of the energy $E_h(\mathbf{h})$ (normalized to \bar{E}_h) are depicted in Fig. 10 for all four profiles. It is clearly visible that diversity increases in the order RA, TU, HT, and EQ. For EQ, very small energies are quite rare, whereas they occur frequently for RA, where an approximately exponential distribution results.

Finally, the pdf of the product $d_{\min}^2(\mathbf{h})/d_{\min, \text{AWGN}}^2 \cdot E_h(\mathbf{h})/\bar{E}_h$ is shown in Fig. 11, which primarily is of interest for performance evaluation (17). Obviously, the distributions are very similar to those for $E_h(\mathbf{h})/\bar{E}_h$. This fact together with the results for the normalized squared Euclidean distance according to Fig. 9 indicate that performance is mainly influenced by fading, not by ISI, if proper equalization schemes are applied.

E. System Performance Including Channel Estimation and Channel Coding

In the following, the proposed equalization concept is applied to an Enhanced General Packet Radio Service (EGPRS) transmission, which is part of the EDGE standard. Nine modulation and coding schemes (MCSs) are specified for EGPRS [48]. Four schemes (MCS-1–MCS-4) employ GMSK modulation, which is also applied in GSM. For good channel conditions, a higher throughput can be achieved with MCS-5–MCS-9, which are based on 8PSK modulation and characterized by individual code rates. Each 8PSK scheme employs the same convolutional code with code rate 1/3. In order to obtain the desired code rate, puncturing is applied. For the following simulation results, we select MCS-5 and MCS-7, corresponding to a data code rate¹¹ of 0.37 and 0.76, respectively. Each encoded block is interleaved and assigned to two or four bursts, depending on the selected MCS (MCS-5, MCS-7: 4 bursts). Each burst consists of 2×58 data symbols, 26 training symbols, which are located in the middle of the burst (midamble), and three tail symbols at either end. The interleaving tables of the EDGE standard have been carefully optimized. Using different tables may entail a significant performance degradation.

For receiver input filtering, an SRC filter with rolloff factor $\alpha = 0.3$ has been selected Section IV-C. Because additional reliability information is highly beneficial for channel decoding, a BCJR-type soft-output RSSE algorithm as proposed in [20] and [21] is used for equalization. A state number of $Z = 2$ is chosen (RSSE2), which seems to be especially interesting for a practical implementation with only moderate complexity. Two different equalization processes are performed. Both start from the midamble, the first one proceeds in negative time direction and the second one in positive time direction also [49]. For channel estimation, the standard ML approach [43] is adopted. In order

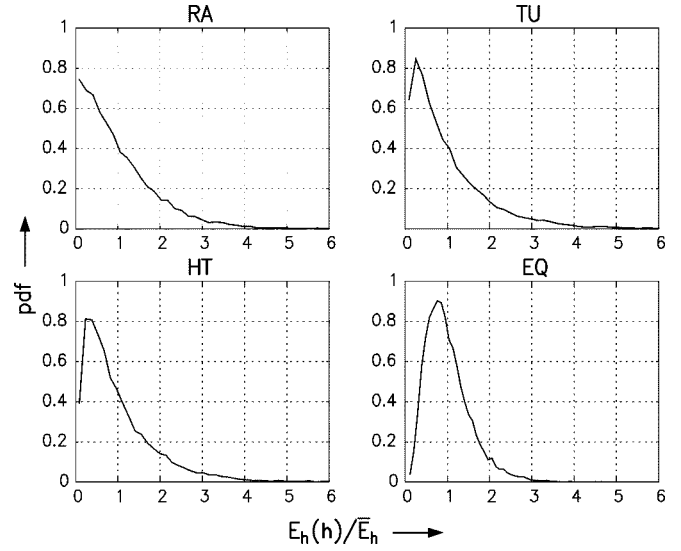


Fig. 10. Pdf's of $E_h(\mathbf{h})/\bar{E}_h$ for different channel profiles.

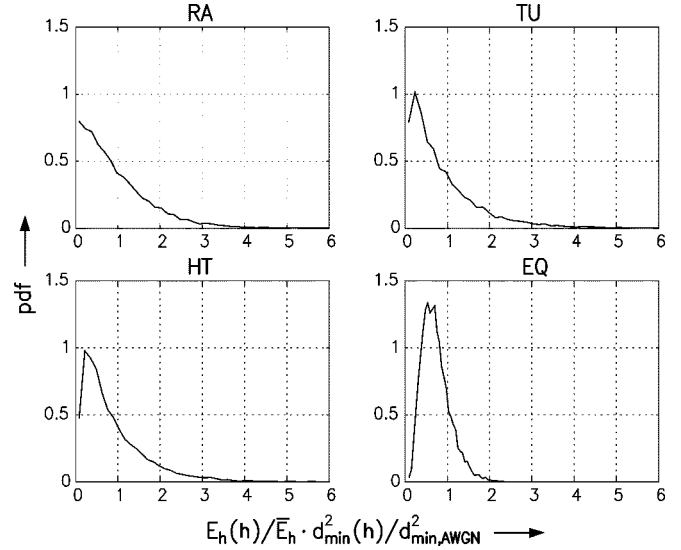


Fig. 11. Pdf's of $E_h(\mathbf{h})/\bar{E}_h \cdot d_{\min}^2(\mathbf{h})/d_{\min, \text{AWGN}}^2$ for MLSE and different channel profiles.

to (approximately) transform the CIR into its minimum-phase equivalent, a fixed FIR prefilter is calculated for each burst via the LP approach [30], [31], which uses the estimated channel impulse response. For tracking of the time-variant discrete-time overall channel impulse response, the least-mean-square (LMS) algorithm [50] is employed.

Fig. 12 shows the resulting BERs after channel decoding versus $10\log_{10}(\bar{E}_b/N_0)$ for the TU3 profile, where “3” indicates a velocity of the mobile station of $v = 3$ km/h. Frequency hopping has been used in order to obtain a high diversity for channel coding. For each of the four bursts contained in a block, a different frequency is used. Hence, the channel impulse responses of different bursts in a block are mutually statistically independent and interleaving is highly beneficial. At $\text{BER} = 10^{-3}$, MCS-5 performs ≈ 4.8 dB better than MCS-7. On the other hand, MCS-7 is twice as efficient as MCS-5 in terms of information bit rate (MCS-7: 44.8 kb/s, MCS-5: 22.4 kb/s). A comparison of Figs. 3 and 12 shows

¹⁰This in general tends to hold for randomly generated CIRs with approximately evenly distributed energy over the whole time span, as further calculations have shown.

¹¹For encoding of header information, different code rates are used.

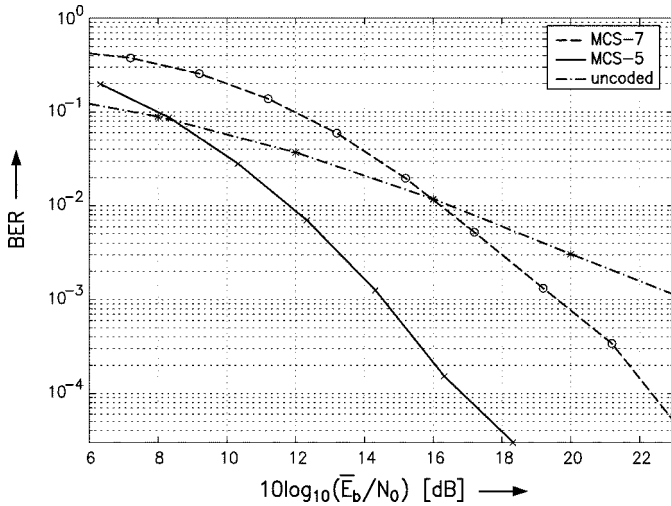


Fig. 12. BER after channel decoding versus $10 \log_{10}(\bar{E}_b/N_0)$ for RSSE2 for TU3 profile (MCS-5 and MCS-7, frequency hopping, imperfect channel estimation). BER of uncoded transmission is also shown for comparison.

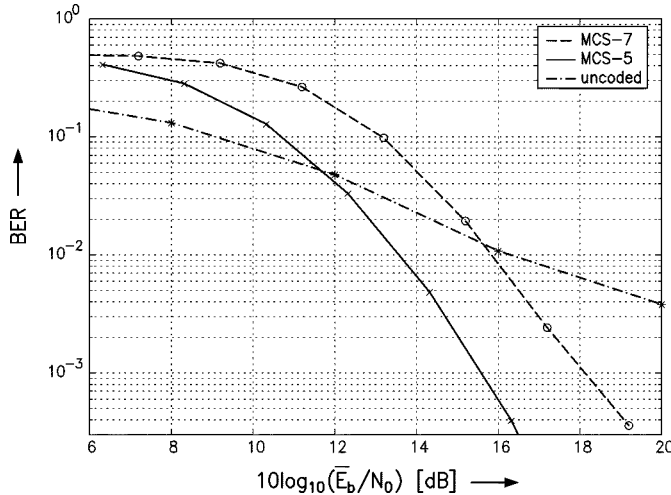


Fig. 13. BER after channel decoding versus $10 \log_{10}(\bar{E}_b/N_0)$ for RSSE2 for EQ50 profile (MCS-5 and MCS-7, frequency hopping, imperfect channel estimation). BER of uncoded transmission is also shown for comparison.

that powerful channel coding yields a significant improvement in power efficiency. Without channel coding, but with ideal channel estimation, $10 \log_{10}(\bar{E}_b/N_0) = 21.4$ dB is required for $\text{BER} = 10^{-3}$, i.e., MCS-5 yields a gain of ≈ 7 dB. Fig. 12 contains also a simulated BER curve for uncoded transmission with imperfect channel estimation which confirms the results of Fig. 3 and indicates a loss due to channel estimation errors of ≈ 1.6 dB at $\text{BER} = 10^{-3}$. This loss is in good accordance with the theoretical analysis of Section IV-B.

Fig. 13 shows BER versus $10 \log_{10}(\bar{E}_b/N_0)$ for the EQ50 profile. Frequency hopping has not been applied, i.e., the same frequency is used for each burst belonging to a block. Therefore, the available diversity is limited and the potential gain of channel coding together with interleaving is lower than for the previous example. Because of the velocity of $v = 50$ km/h, a direct comparison with the results of Section IV-A is not possible for which time invariance of the channel during each burst has been assumed. Imperfect LMS channel tracking causes a loss

for $v \neq 0$ km/h especially at low BERs. Also, nonideal prefiltering causes a performance loss especially for long nonminimum-phase CIRs, which frequently arise for the EQ profile. All the described effects cannot be avoided in a practical receiver. They explain why the simulated BER curve for uncoded transmission of Fig. 13 is worse than the results presented in Fig. 4 for which practical effects are not taken into account.

Hence, the results presented in Section IV can serve as guidelines for the design of equalization for EDGE, but they cannot replace a detailed simulation of a practical receiver including all nonideal effects and components.

V. CONCLUSION

In this paper, equalization for EDGE has been considered. Because of the high-level modulation applied in EDGE, in contrast to GSM, MLSE cannot be employed for equalization in a practical scheme. As has been demonstrated by analytical and simulation results, DDFSE or RSSE with only a few number of states together with prefiltering are attractive solutions. A state number of $Z = 8$ for DDFSE and of $Z = 2$ or $Z = 4$ for RSSE seems to be sufficient for a performance rather close to the theoretical limit given by the performance of MLSE. Furthermore, it has been shown that a receiver input filter with an SRC frequency response performs close to the optimum WMF, while complexity is significantly lower. Also, it has been demonstrated via pdf's of the minimum Euclidean distance that the performance loss compared to the AWGN channel is mainly caused by fading, not by ISI, if well-designed trellis-based equalizers are applied. Finally, the effects of channel coding and channel estimation have been considered. It is shown that the loss due to ML channel estimation is limited, however, especially at high vehicle speeds imperfect tracking of the CIR causes a considerable degradation which may be compensated by powerful channel coding.

REFERENCES

- [1] A. Furuskär, S. Mazur, F. Müller, and H. Olofsson, "EDGE: Enhanced data rates for GSM and TDMA/136 evolution," *IEEE Pers. Commun.*, vol. 6, pp. 56–66, June 1999.
- [2] R. van Nobelen, N. Seshadri, J. Whitehead, and S. Timiri, "An adaptive radio link protocol with enhanced data rates for GSM evolution," *IEEE Pers. Commun.*, vol. 6, pp. 54–63, Feb. 1999.
- [3] A. Duel and C. Heegard, "Delayed decision-feedback sequence estimation," in *Proc. 23rd Annu. Allerton Conf. Communications, Control, Computing*, Oct. 1985.
- [4] A. Duel-Hallen and C. Heegard, "Delayed decision-feedback sequence estimation," *IEEE Trans. Commun.*, vol. 37, pp. 428–436, May 1989.
- [5] M. V. Eyuboğlu and S. U. Qureshi, "Reduced-state sequence estimation with set partitioning and decision feedback," *IEEE Trans. Commun.*, vol. 36, pp. 13–20, Jan. 1988.
- [6] —, "Reduced-state sequence estimation for coded modulation on intersymbol interference channels," *IEEE J. Select. Areas Commun.*, vol. 7, pp. 989–995, Aug. 1989.
- [7] P. R. Chevillat and E. Eleftheriou, "Decoding of trellis-encoded signals in the presence of intersymbol interference and noise," *IEEE Trans. Commun.*, vol. 37, pp. 669–676, July 1989.
- [8] J. B. Anderson and S. Mohan, "Sequential coding algorithms: A survey and cost analysis," *IEEE Trans. Commun.*, vol. COM-32, pp. 169–176, Feb. 1984.
- [9] G. Foschini, "A reduced state variant of maximum likelihood sequence detection attaining optimum performance for high signal-to-noise ratios," *IEEE Trans. Inform. Theory*, vol. IT-23, pp. 605–609, Sept. 1977.
- [10] P. Monsen, "Feedback equalization for fading dispersive channels," *IEEE Trans. Info. Theory*, vol. IT-17, pp. 56–64, Jan. 1971.

- [11] C. A. Belfiore and J. H. Park, "Decision-feedback equalization," *Proc. IEEE*, vol. 67, pp. 1143–1156, Aug. 1979.
- [12] R. W. Lucky, J. Salz, and E. J. Weldon Jr., *Principles of Data Communication*. New York: McGraw-Hill, 1968.
- [13] "Tdoc SMG2 WPB 325/98," ETSI, Nov. 1998.
- [14] P. Jung, "Laurent's representation of binary digital continuous phase modulated signals with modulation index 1/2 revisited," *IEEE Trans. Commun.*, vol. 42, pp. 221–224, Feb.–Apr. 1994.
- [15] H. Olofsson and A. Furuskär, "Aspects of introducing EDGE in existing GSM networks," in *Proc. IEEE Int. Conf. Universal Personal Communications*, 1998, pp. 421–426.
- [16] "GSM Recommendations 05.05 Version 5.3.0," ETSI, Dec. 1996.
- [17] G. D. Forney Jr., "Maximum-likelihood sequence estimation of digital sequences in the presence of intersymbol interference," *IEEE Trans. Info. Theory*, vol. IT-18, pp. 363–378, May 1972.
- [18] J. G. Proakis, *Digital Communications*, 3rd ed. New York: McGraw-Hill, 1995.
- [19] C. Lusch, M. Sandell, P. Strauch, and R.-H. Yan, "Adaptive channel memory truncation for TDMA digital mobile radio," in *Proc. IEEE Int. Workshop Intelligent Signal Processing and Communication Systems*, Melbourne, Australia, Nov. 1998, pp. 665–669.
- [20] W. Koch and A. Baier, "Optimum and sub-optimum detection of coded data disturbed by time-varying intersymbol interference," in *Proc. IEEE Global Telecommunication Conf.*, San Diego, CA, Dec. 1990, pp. 807.5.1–807.5.6.
- [21] P. Höher, "TCM on frequency-selective fading channels: A comparison of soft-output probabilistic equalizers," in *Proc. IEEE Global Telecommunication Conf.*, San Diego, CA, Dec. 1990, pp. 401.4.1–401.4.6.
- [22] S. Müller, W. Gerstacker, and J. Huber, "Reduced-state soft-output trellis-equalization incorporating soft feedback," in *Proc. IEEE Global Telecommunication Conf.*, London, U.K., Nov. 1996, pp. 95–100.
- [23] L. R. Bahl, J. Cocke, F. Jelinek, and J. Raviv, "Optimal decoding of linear codes for minimizing symbol error rate," *IEEE Trans. Info. Theory*, vol. IT-20, pp. 284–287, Mar. 1974.
- [24] L.-N. Lee, "Real-time minimal-bit-error probability decoding of convolutional codes," *IEEE Trans. Commun.*, vol. COM-22, pp. 146–151, 1974.
- [25] R. Raheli, A. Polydoros, and C.-K. Tzou, "Per-survivor processing: A general approach to MLSE in uncertain environments," *IEEE Trans. Commun.*, vol. 43, pp. 354–364, Feb.–Apr. 1995.
- [26] W. Gerstacker and J. Huber, "Improved equalization for GSM mobile communications," in *Proc. Int. Conf. Telecommunications*, Istanbul, Apr. 1996, pp. 128–131.
- [27] M. Schmidt and G. P. Fettweis, "FIR prefiltering for near minimum phase target channels," in *Proc. 6th Canadian Workshop Information Theory*, June 1999.
- [28] B. Yang, "An improved fast algorithm for computing the MMSE decision-feedback equalizer," *Int. J. Electron. Commun.*, vol. 53, no. 1, pp. 1–6, 1999.
- [29] N. Al-Dhahir and J. M. Cioffi, "Fast computation of channel-estimate based equalizers in packet data transmission," *IEEE Trans. Signal Processing*, vol. 43, pp. 2462–2473, Nov. 1995.
- [30] W. Gerstacker and F. Obernosterer, "Process and Apparatus for Receiving Signals Transmitted Over a Distorted Channel," Eur. Patent 99301299.6, Feb. 1999.
- [31] W. H. Gerstacker, F. Obernosterer, R. Meyer, and J. B. Huber, "An efficient method for prefilter computation for reduced-state equalization," in *Proc. IEEE Int. Symp. Personal, Indoor, and Mobile Radio Communications*, London, U.K., Sept. 2000, pp. 604–609.
- [32] J. Makhoul, "Linear prediction: A tutorial review," *Proc. IEEE*, vol. 63, pp. 561–580, Apr. 1975.
- [33] T. Larsson, "A state-space partitioning approach to trellis decoding," Chalmers Univ. Technology, Göteborg, Sweden, Tech. Rep. 222, 1991.
- [34] B. Spinnler and J. Huber, "Design of hyper states for reduced-state sequence estimation," in *Proc. Int. Conf. Communications*, Seattle, WA, June 1995, pp. 1–6.
- [35] E. Horowitz and S. Sahni, *Fundamentals of Data Structures*. New York: Pitman, 1976.
- [36] J. Huber, *Trelliscodierung in der Digitalen Übertragungstechnik—Grundlagen und Anwendungen* (in German). Berlin, Germany: Springer-Verlag, 1992.
- [37] J. M. Cioffi, "An error event length conjecture," in *Proc. Conf. Specific Problems in Communication and Computation*, Palo Alto, CA, Sept. 1986.
- [38] J. M. Cioffi and C. M. Melas, "Evaluating the performance of maximum likelihood sequence detection in a magnetic recording channel," in *Proc. IEEE Global Telecommunication Conf.*, Houston, TX, Dec. 1986, pp. 1066–1070.
- [39] S. Benedetto, E. Biglieri, and V. Castellani, *Digital Transmission Theory*. Englewood Cliffs, NJ: Prentice-Hall, 1987.
- [40] P. J. Davis and P. Rabinowitz, *Methods of Numerical Integration*, 2nd ed. San Diego, CA: Academic, 1984.
- [41] W. H. Gerstacker and R. Schöber, "Analytical results on the statistical distribution of the zeros of mobile channels," in *Proc. IEEE Int. Symp. Personal, Indoor, and Mobile Radio Communications*, London, U.K., Sept. 2000, pp. 304–309.
- [42] R. Schöber and W. H. Gerstacker, "On the distribution of zeros of mobile channels with application to GSM/EDGE," *IEEE J. Select. Areas Commun.*, vol. 19, pp. 1289–1299, July 2001.
- [43] S. N. Crozier, D. D. Falconer, and S. A. Mahmoud, "Least sum of squared errors (LSSE) channel estimation," *Inst. Elect. Eng. Proc.-F*, vol. 138, pp. 371–378, Aug. 1991.
- [44] K.-H. Chang and C. N. Georghiades, "Iterative joint sequence and channel estimation for fast time-varying intersymbol interference channels," in *Proc. Int. Conf. Communications*, Seattle, WA, June 1995, pp. 357–361.
- [45] S. A. Fichtel and H. Meyr, "Optimal parametric feedforward estimation of frequency-selective fading radio channels," *IEEE Trans. Commun.*, vol. 42, pp. 1639–1650, Feb.–Apr. 1994.
- [46] A. Gorokhov, "On the performance of the Viterbi equalizer in the presence of channel estimation errors," *IEEE Signal Processing Lett.*, vol. 5, pp. 321–324, Dec. 1998.
- [47] K. A. Hamied and G. L. Stüber, "An adaptive truncated MLSE receiver for Japanese personal digital cellular," *IEEE Trans. Veh. Technol.*, vol. 45, pp. 41–50, Feb. 1996.
- [48] S. Nanda, K. Balachandran, and S. Kumar, "Adaptation techniques in wireless packet data services," *IEEE Commun. Mag.*, vol. 38, pp. 54–64, Jan. 2000.
- [49] S. Ariyavisitakul, "A decision feedback equalizer with time-reversal structure," *IEEE J. Select. Areas Commun.*, vol. 10, pp. 599–613, Apr. 1992.
- [50] S. Haykin, *Adaptive Filter Theory*, 3rd ed. Englewood Cliffs, NJ: Prentice-Hall, 1996.



Wolfgang H. Gerstacker (S'93–A'98–M'99) was born in Nürnberg, Germany, in 1966. He received the Dipl.-Ing. and Dr.-Ing. degrees in electrical engineering from the University of Erlangen-Nürnberg, Erlangen, Germany, in 1991 and 1998, respectively.

From 1992 to 1998, he was a Research Assistant with the Telecommunications Institute of the University of Erlangen-Nürnberg. Since 1998, he has been a Consultant for mobile communications and a Lecturer in digital communications with the University of Erlangen-Nürnberg. From 1999 to 2000, he was a

Visiting Research Fellow with the University of Canterbury, Christchurch, New Zealand, sponsored by a fellowship from the German Academic Exchange Service (DAAD). His current research interests include equalization and channel estimation, blind techniques, space-time coding, and noncoherent detection algorithms.

Robert Schöber (S'98) was born in Neuendettelsau, Germany, in 1971. He received the Diplom (Univ.) and Dr.-Ing. degrees in electrical engineering from the University of Erlangen-Nürnberg, Erlangen, Germany, in 1997 and 2000, respectively.

During his studies, he was supported by a scholarship of the "Studienstiftung des deutschen Volkes." From November 1997 to May 2001, he was a Research and Teaching Assistant with the Telecommunications Institute II (Digital Transmission and Mobile Communications), University of Erlangen-Nürnberg. Since May 2001, he has been a Postdoctoral Fellow with the University of Toronto, Toronto, ON, Canada, sponsored by a fellowship from the German Academic Exchange Service (DAAD). His current research interests are in the area of noncoherent detection, equalization, space-time coding, and multiuser detection.